Supporting Information

Electronic State-Resolved Multimode-Coupled Vibrational Wavepackets in Oxazine 720 by Two-Dimensional Electronic Spectroscopy

Ruidan Zhu[1,2], Jiading Zou[1,2], Zhuan Wang[1], Hailong Chen[1,3], Yuxiang Weng[1,2,3,]*

[1]Beijing National Laboratory for Condensed Matter Physics, Laboratory of Soft Matter Physics, Institute of Physics, Chinese Academy of Sciences, Beijing 100190, China

[2]University of Chinese Academy of Sciences, Beijing 100049, China

[3]Songshan Lake Materials Laboratory, Dongguan, Guangdong 523808, China

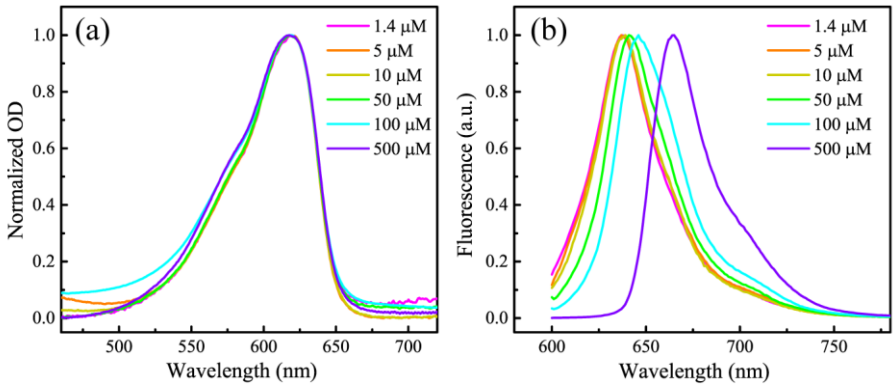

Figure S1. The concentration-dependent absorption (a) and fluorescence (b) spectra of oxazine 720 in methanol.

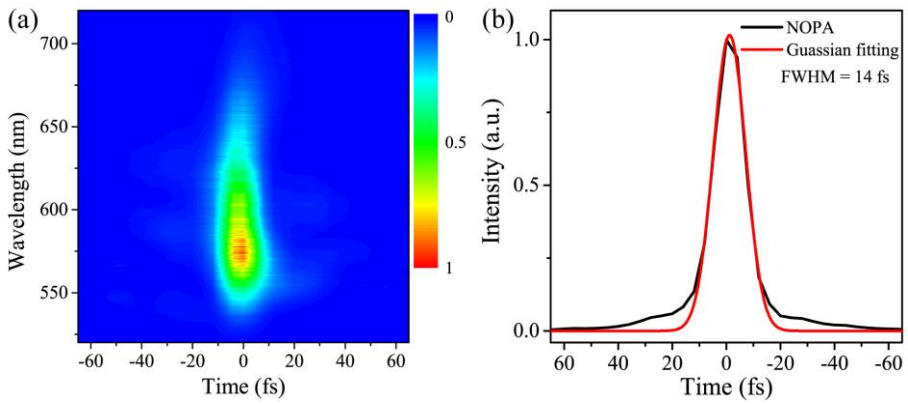

Figure S2. The pulse measurement of NOPA via transient grating frequency-resolved

optical gating (TG-FROG)[1]. (a) TG-FROG map recorded in the same experimental condition of 2DES and HD-TG experiments. (b) The integrated TG-FROG trace along wavelength axis (black) fitted by a Gaussian function (red) with ~14 fs full width at half-maximum (FWHM), leading to a pulse duration of 11.5 fs.

Data processing procedure

The spectral interference fringes recorded at each waiting time were Fourier filtered using a Hamming window in the inverse Fourier domain (i.e., t_3 domain), centered at 430 fs with the window size of 200 fs. After Fourier transform back into the frequency domain, the amplitude of TG/2DES signals is divided by the square root of LO intensity and then multiplied with a phase factor associated with the time delay between LO and the third pulse to remove the linear spectral phase. Finally, the 2DES signals are retrieved in the frequency domain via Fourier transform along the coherence time τ.

The pure absorptive 2D maps were phased using the projection slice theorem with two phase factors (φ: phase constant; t_c: time delay between beam 3 and the LO) to match the frequency-resolved pump-probe results[2]. The optimization procedure converges when the sum of the squared difference between the normalized projection of the 2D spectrum onto ω_3 axis and the normalized pump-probe spectrum is minimal. The representative phased 2D spectrum and the comparison of the corresponding projection onto ω_3 with pump-probe results at T = 240 fs are shown in Figure S3. The TG data in Fig. S4(a) were phased using the same phasing procedure at each waiting time.

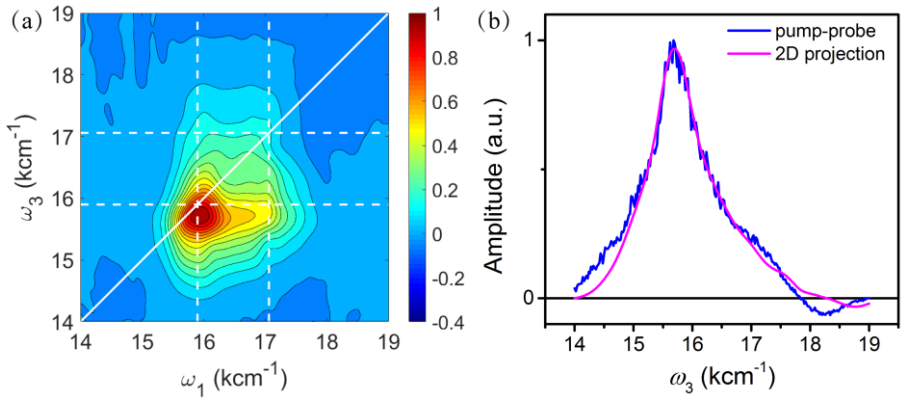

Figure S3. (a) The representative absorptive 2D spectrum at T = 240 fs. The dashed

lines indicate the two absorption peaks (ω_1=15900 cm^{-1} and 17060 cm^{-1}). (b) The comparison of the projection of 2D spectrum (magenta) onto ω_3 with the corresponding pump-probe spectrum (blue).

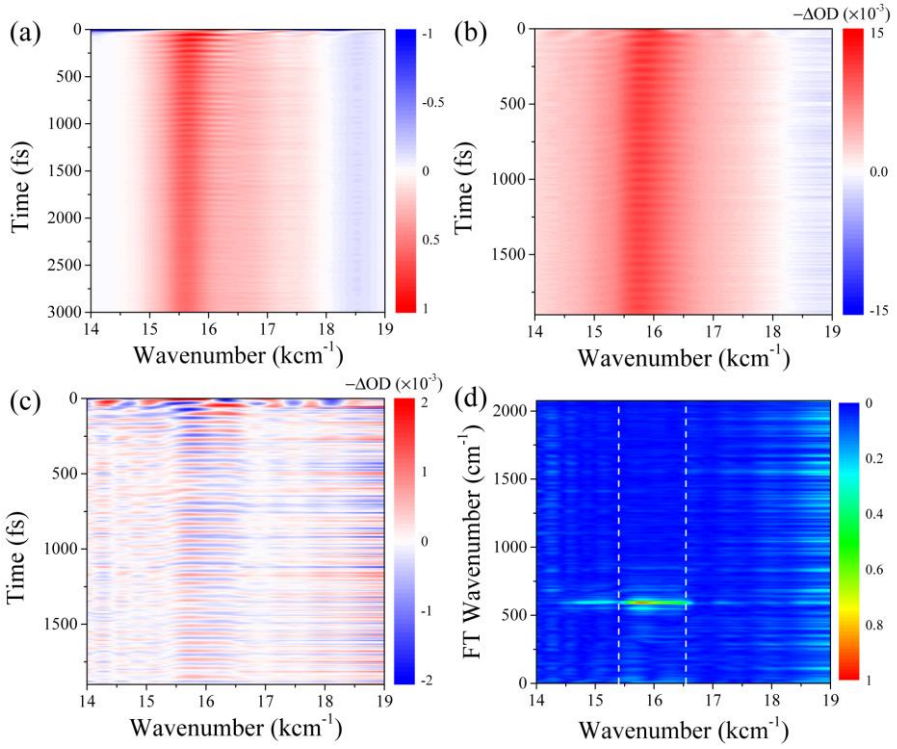

Figure S4. (a) The HD-TG spectrum of oxazine 720 in methanol without removal of the population decays. (b) BBTA spectrum from 0 to 1.9 ps. The amplitude of the data corresponds to the absorption change (ΔOD) after photo-excitation. The scattering contributions were removed by a FT filtering algorithm[3]. The red color indicates the signals of ground state bleaching (GB) and stimulated emission (SE), while the blue color represents the signals of excited state absorption (ESA). (c) The residual BBTA spectrum after global fitting. (d) The corresponding Fourier transform map of (c). The dashed line shows the position of nodes.

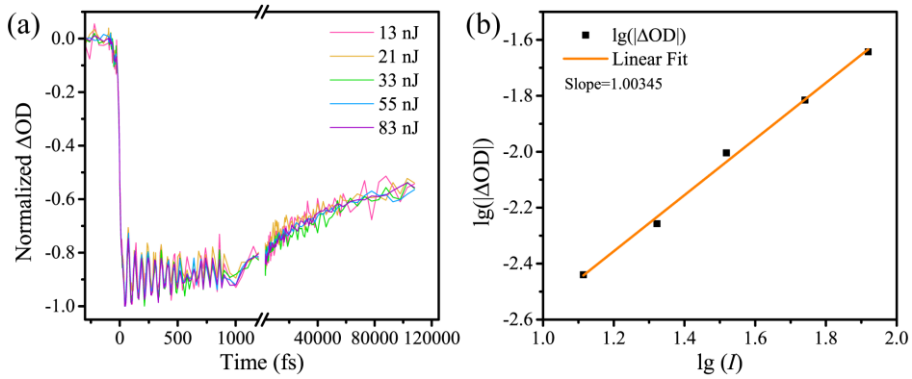

Figure S5. Intensity-dependent BBTA measurements using the excitation spectrum shown in Fig. 1(a) in the main text. (a) The normalized dynamics at the emission wavelength of 633 nm measured with different pulse energies and scanned up to 120 ps. (b) The excitation-induced absorption change ΔOD (black squares) averaged from 627 nm to 633 nm at T = 100 fs as a function of pulse energy, which can be well fitted with linear function. The linear relation indicates the dynamics of transient signals are almost independent of excitation intensity.

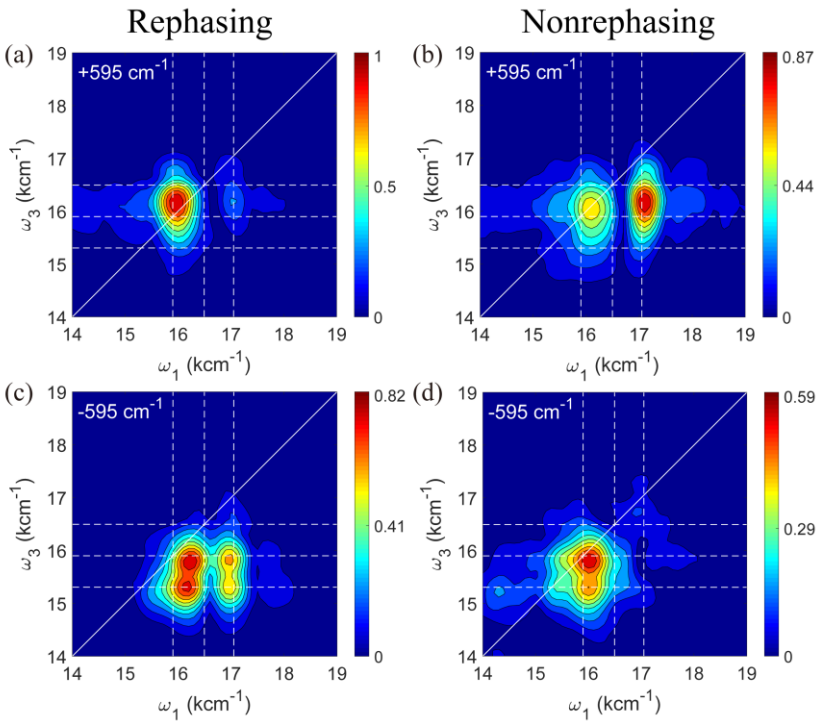

Figure S6. FT maps of ν = ±595 cm^{-1} for rephasing (a)-(b) and nonrephasing (c)-(d) signals at the 10 μM concentration of oxazine 720 in methanol. The white dashed lines vertical to the excitation axis denote the transition frequencies at E_0 (15900 cm^{-1}), E_0

+595 cm^{-1} and E_0 +1150 cm^{-1} respectively, while the dashed lines vertical to the emission axis denote the frequencies at E_0 and $E_0 \pm 595$ cm^{-1}. The FT amplitude is seven times weaker than those in Fig. 3.

Time-frequency transform for oscillating signals

The smoothed-pseudo-Wigner-Ville (SPWV) distribution was first used to analyze coherent signals in 2D spectroscopy by Volpato and Collini[4]. Compared to continuous wavelet transform (CWT), SPWV has less apparent edge effects and gets more accurate dynamic information at early time. As mentioned in Ref. 4, the parameters of window function are crucial for time-frequency transform to obtain the satisfying temporal and frequency resolutions. To retrieve time-frequency information of oscillation signals lasting for ~1ps, we use Gaussian window function, i.e.,

$$h(t) = \exp(-t^2 / 2\sigma_h^2)$$
$$g(t) = \exp(-t^2 / 2\sigma_g^2) \quad \text{(S1)}$$

as the smooth windows in SPWV transform. Parameters $\sigma_h = \sigma_g = 360$ fs are chosen to balance the time-frequency resolution. Smaller σ will result in larger broadening at frequency axis and cause obvious interference when two frequency components are close to each other. If σ is too large, dephasing time becomes much inaccurate and smoothing effect would be poor. The recommended window parameters in SPWV transform are determined when the resulting spectral broadening close to the actual broadening in Fourier transform (FT).

The oscillation signals in real-part rephasing maps are used and simulated by a damped oscillation model which is described as:

$$S(t) = a_1 \exp(-t/\tau_1)\cos(2\pi\nu_1 t + \varphi_1) + a_2 \exp(-t/\tau_2)\cos(2\pi\nu_2 t + \varphi_2), \quad \text{(S2)}$$

where ν_1 and ν_2 are oscillation frequencies, φ_1 and φ_2 are the initial phases, a_1 and a_2 are oscillation amplitudes and τ_1, τ_2 are dephasing times. The SPWV results from 40 fs to 3200 fs in experiment and simulation are shown in Figure S7. Oscillation frequencies ν_1 = 595 cm^{-1} and ν_2 =555 cm^{-1} are determined by FT results. φ_1 and φ_2 are assumed to zero for simplicity. Approximate dephasing times τ_1 = 1300 fs and τ_2 = 600 fs are

determined by the comparison between the experimental and simulated dynamics slices at frequencies v_1 = 595 cm^{-1} and v_2 = 555 cm^{-1} on the SPWV transform maps. Finally, a_1: a_2 ≈ 1:1 are obtained by matching the simulated FT amplitudes to experimental FT results as shown in Fig. S7(d).

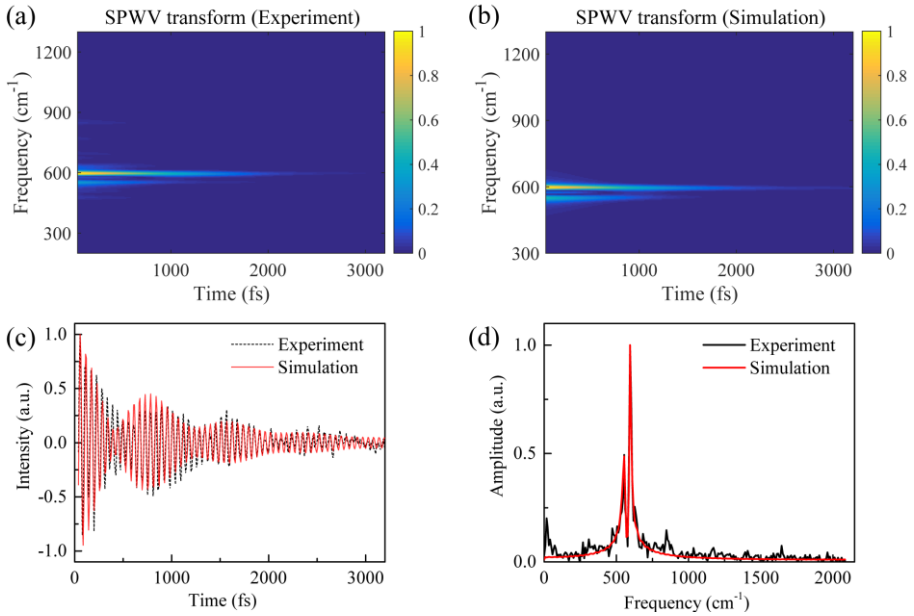

Figure S7. (a) Time-frequency amplitude map of SPWV transform using experimental data at excitation frequency ω_1 = 15900 cm^{-1} and emission frequency ω_3 = 15300 cm^{-1}. (b) The corresponding simulation result obtained by using two damped cosine functions with oscillation frequencies equal to 595 cm^{-1} and 555 cm^{-1}. (c) Time domain traces of experimental and simulated results. (d) FT results of data at (c).

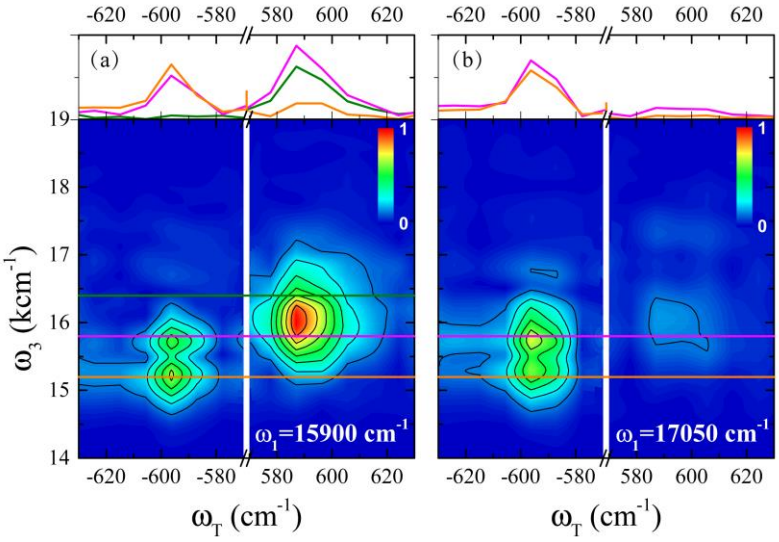

Figure S8. The 2D amplitude cuts of 3D rephasing Fourier maps at ω_1 = 15900 cm^{-1} (a) and 17050 cm^{-1} (b). ω_T is the oscillation frequency along waiting time axis. The slices along the specific emission frequency (orange, green and magenta) on 2D maps indicate the peak positions of oscillation frequency at -595 and 586 cm^{-1}.

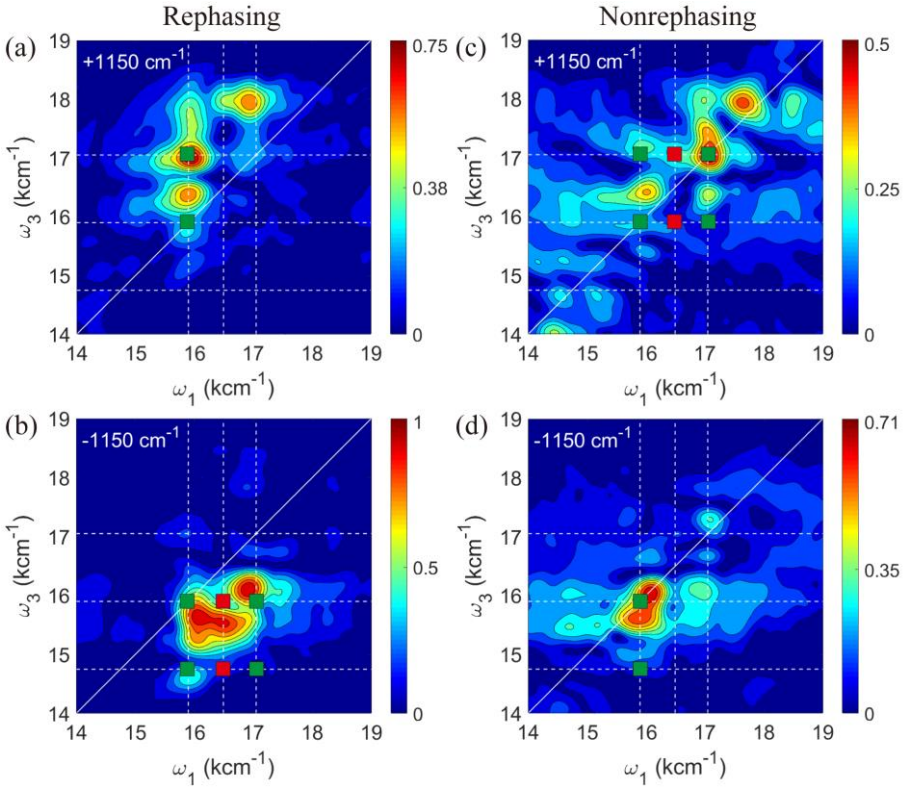

Figure S9. FT maps of v = ±1150 cm^{-1} for rephasing (a)-(b) and nonrephasing (c)-(d) signals. The white dashed lines denote the frequencies of the transition energy at E_0 (15900 cm^{-1}), E_0 +595 cm^{-1} and E_0 ±1150 cm^{-1}. The green squares represent the expected "chair" pattern, while the red ones represent the locations of the expected coupling signals.

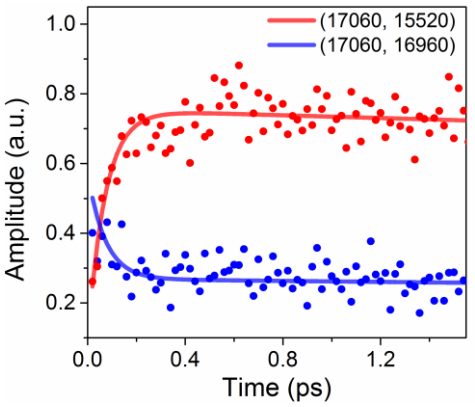

Figure S10. The dynamics slice of vibronic relaxation at ω_1 = 17050 cm^{-1} with the results of global fitting. The lines correspond to the two-exponential fit. The faster component is about 70 fs while a slower process (>> 4 ps) is beyond the range we measured.

Reference

1. Trebino, R.; DeLong, K. W.; Fittinghoff, D. N.; Sweetser, J. N.; Krumbügel, M. A.; Richman, B. A.; Kane, D. J. Measuring Ultrashort Laser Pulses in the Time-Frequency Domain Using Frequency-Resolved Optical Gating. *Rev. Sci. Instrum.* **1997,** *68* (9), 3277-3295.
2. Zhu, R.; Yue, S.; Li, H.; Leng, X.; Wang, Z.; Chen, H.; Weng, Y. Correction of Spectral Distortion in Two-Dimensional Electronic Spectroscopy Arising from the Wedge-Based Delay Line. *Opt. Express* **2019,** *27* (11), 15474.
3. Dean, J. C.; Rafiq, S.; Oblinsky, D. G.; Cassette, E.; Jumper, C. C.; Scholes, G. D. Broadband Transient Absorption and Two-Dimensional Electronic Spectroscopy of Methylene Blue. *J. Phys. Chem. A* **2015,** *119* (34), 9098-108.
4. Volpato, A.; Collini, E. Time-Frequency Methods for Coherent Spectroscopy. *Opt. Express* **2015,** *23* (15), 20040-50.